

On the significance of the area under the after-effect function curve of a magnetic fluid

This article has been downloaded from IOPscience. Please scroll down to see the full text article.

2008 J. Phys.: Condens. Matter 20 204108

(<http://iopscience.iop.org/0953-8984/20/20/204108>)

View [the table of contents for this issue](#), or go to the [journal homepage](#) for more

Download details:

IP Address: 129.252.86.83

The article was downloaded on 29/05/2010 at 12:00

Please note that [terms and conditions apply](#).

On the significance of the area under the after-effect function curve of a magnetic fluid

P C Fannin¹, C N Marin² and C Couper¹

¹ Department of Electronic and Electrical Engineering, Trinity College, Dublin 2, Republic of Ireland

² Faculty of Physics, West University of Timisoara, B-dul V Parvan, no. 4, 300223 Timisoara, Romania

E-mail: pfannin@tcd.ie

Received 1 April 2008

Published 1 May 2008

Online at stacks.iop.org/JPhysCM/20/204108

Abstract

The after-effect function, $b(t)$, describes how the magnetization of a dissipative magnetic fluid decreases with time when a polarizing field, H , is suddenly removed. It is shown that with increasing H , the rate of decay of $b(t)$ increases and also that the area, $\int_0^\infty b(t) dt = B$, under each decay curve decreases. Here we investigate the significance of this and by means of a simple model, show that the normalized function, $B/b(0)$, is in fact equal to the Debye relaxation time τ_D . The results of applying the model to theoretically generated data and also to data obtained from a magnetic fluid sample are presented.

1. Introduction

The after-effect function, $b(t)$, or magnetization decay function of a magnetic fluid, represents the decay of magnetization after the removal of an external polarizing magnetic field and can be related to the frequency dependent complex susceptibility, $\chi(\omega) = \chi'(\omega) - i\chi''(\omega)$.

$b(t)$ [1, 2] may be obtained from the imaginary, or dissipative component, $\chi''(\omega)$, by means of the equation

$$\frac{\chi''(\omega)}{\omega} = \frac{1}{2} \operatorname{Re} \left\{ \int_{-\infty}^{\infty} b(t) \exp(-i\omega t) dt \right\}. \quad (1)$$

The component of equation (1) within the brackets is in fact the Fourier transform of $b(t)$; thus $b(t)$ can be obtained by carrying out an inverse Fourier transformation (F^{-1}) on $\chi''(\omega)/\omega$, where

$$b(t) = 2 \operatorname{Re} [F^{-1} \{ \chi''(\omega)/\omega \}]. \quad (2)$$

Now, there are two distinct mechanisms by which the magnetization of magnetic fluids may relax after an applied field has been removed: either by rotational Brownian motion of the particle within the carrier liquid, with its magnetic moment, m , locked in an axis of easy magnetization, or by rotation of the magnetic moment within the particle. The

time associated with the rotational diffusion is the Brownian relaxation time τ_B [3] where

$$\tau_B = 3V\eta/kT. \quad (3)$$

V is the hydrodynamic volume of the particle, η is the dynamic viscosity of the carrier liquid, k is Boltzmann's constant and T is the temperature of the system.

In the case of the second relaxation mechanism, the magnetic moment may reverse direction within the particle by overcoming an energy barrier, which, for uniaxial anisotropy, is given by Kv , where K is the anisotropy constant of the particle and v is the magnetic volume of the particle. The probability of such a transition is proportional to $\exp(\sigma)$ where $\sigma = kv/KT$ is the ratio of anisotropy energy to thermal energy. This reversal time is characterized by a time τ_N , which is referred to as the Néel relaxation time [4], and given by the expression

$$\tau_N = \tau_0 \exp(\sigma). \quad (4)$$

τ_0 is a decay time, often quoted as having an approximate value of 10^{-8} – 10^{-10} s [5].

A distribution of particle sizes implies the existence of a distribution of relaxation times, with both relaxation mechanisms contributing to the magnetization. They do so

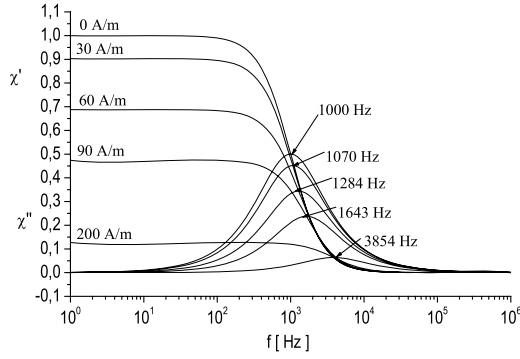


Figure 1. Theoretical plot of $\chi'(\omega H)$ and $\chi''(\omega H)$.

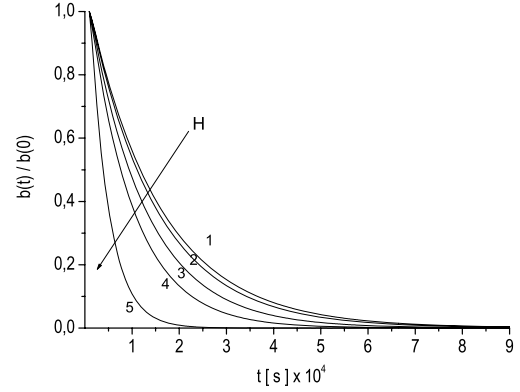


Figure 2. Plot of $b(t)/b(0)$ as a function of H for the data in figure 1.

with an effective relaxation time τ_{eff} [6, 7], where, for a particular particle,

$$\tau_{\text{eff}} = \tau_N \tau_B / (\tau_N + \tau_B) \quad (5)$$

the mechanism with the shortest relaxation time being dominant. In this study, Brownian relaxation is considered to be dominant.

2. The after-effect function and relaxation time in the Debye approximation

The frequency dependent complex susceptibility, $\chi(\omega)$, may be written in terms of its real and imaginary components, where $\chi(\omega) = \chi'(\omega) - i\chi''(\omega)$. The theory developed by Debye [8] to account for the anomalous dielectric dispersion in dipolar fluids has been successfully used [9] to account for the analogous case of magnetic fluids.

According to Debye's theory, the complex susceptibility, $\chi(\omega)$, has a frequency dependence given by the equation

$$\chi(\omega) - \chi_\infty = (\chi_0 - \chi_\infty) / (1 + i\omega\tau_{\text{eff}}) \quad (6)$$

where the static susceptibility, χ_0 , is defined as

$$\chi_0 = nm^2 / 3kT\mu_0 \quad (7)$$

where μ_0 is the permeability of free space and where

$$\tau_{\text{eff}} = 1/\omega_{\text{max}} = 1/2\pi f_{\text{max}}. \quad (8)$$

f_{max} is the frequency at which $\chi''(\omega)$ is a maximum, n is the particle number density and χ_∞ indicates the susceptibility value at very high frequencies (i.e. $f \gg f_{\text{max}}$).

It has been shown that the application of a polarizing field, H , to the sample results in reductions in both $\chi'(\omega)$ and $\chi''(\omega)$ with increasing biasing field and a corresponding shift in f_{max} to higher frequencies [10]. Assuming a Langevin dependence of the magnetization of the magnetic fluid on the polarizing fields, H , an expression for $\chi(\omega, H)$ can be written as [10]

$$\chi(\omega, H) = g(H)\chi_\infty + \frac{(\chi_0 - \chi_\infty)g(H)}{1 + i\omega\tau_{\text{eff}}} \quad (9)$$

with

$$g(H) = 3 [1 + \xi^{-2} - \coth^2(\xi)] \quad (10)$$

where $\xi = mH/kT$. Applying the polarizing field parallel to the alternating field (i.e. the measurement field), in the rigid dipole approximation, the Brownian relaxation time obeys the theoretical dependence [11]

$$\tau_B(H) = \tau_B \frac{\xi [1 - \coth^2(\xi) + \xi^{-2}]}{\coth(\xi) - \xi^{-1}}. \quad (11)$$

Figure 1 shows plots of theoretically generated Debye type complex susceptibility data for increasing values of polarizing field, H , over the range 0 up to 200 A m⁻¹. One can observe that with increasing H , the low frequency susceptibility, χ_0 , decreases and the frequency of the maximum, f_{max} , increases.

Figure 2 shows the corresponding after-effect functions obtained by application of equations (9)–(11) to equation (2). It clearly shows that, with increasing H , the rate of decay of $b(t)$ increases and also that the area under each decay curve decreases.

Here in this work we ask the question, ‘what is the meaning of the area under the decay curve?’ In pursuit of the answer to this question, we consider the Debye case for which [1]

$$b(t) = b(0) \exp(-t/\tau_D) \quad (12)$$

where τ_D is the relaxation time. The area under the after-effect function is

$$B = b(0) \int_0^\infty \exp(-t/\tau_D) dt = b(0)\tau_D. \quad (13)$$

Consequently this simple analysis shows that the normalized area under the after-effect function, $b(t)$, corresponds to the relaxation time of the particles.

3. Testing the model

The theoretical data shown in figures 1 and 2 were initially used to test the validity of equation (13). Equation (8) shows the relationship between the frequency of the maximum of an absorption peak and the relaxation time. The result of applying this to the absorption peaks of figure 1 is shown in figure 3. We denote by τ_m the relaxation time determined from the relaxation peak by means of equation (8). For comparison

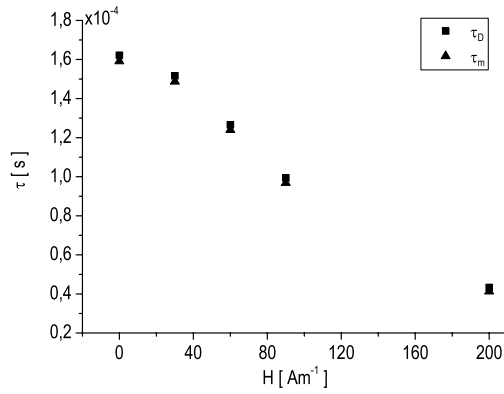


Figure 3. Plot of τ_D and τ_m against H for the theoretical Debye model.

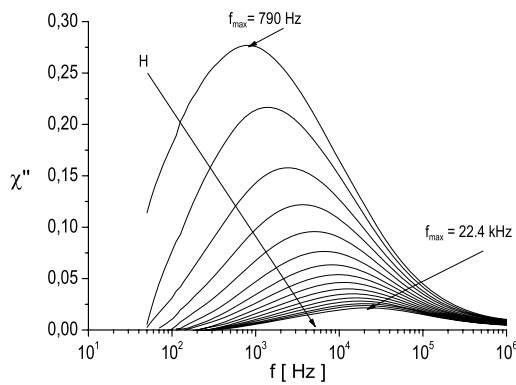


Figure 4. Plot of $\chi''(\omega, H)$ against f (Hz) with f_{max} ranging from 790 Hz to 22.4 kHz.

purposes, the value of $B/b(0) = \tau_D$ was determined for each value of H , and the results obtained are shown in figure 3. We denote by τ_D the relaxation time determined from the area under the plot of $b(t)/b(0)$.

From figure 3 it is readily seen that τ_m and τ_D values are almost identical and therefore confirm the validity of the model for a system with a single relaxation time. The differences between τ_D and τ_m result from the approximation made in the numerical evaluation of the inverse Fourier transform on $\chi''(\omega)/\omega$ and of the integral $\int_0^\infty b(t) dt$.

4. Measurements and results

In order to apply the model to practical measurements, complex magnetic susceptibility measurements, over the frequency range 50 Hz–1 MHz, were made by means of the toroidal technique [12] in conjunction with a Hewlett-Packard RF Bridge 4291A on a colloidal dispersion of cobalt ferrite particles in Isopar M, with a saturation magnetization of 300 G. The particle mean radius was 5 nm, whilst the surfactant was oleic acid.

A high permeability toroid wound with twenty excitation turns was used. A second coil comprising three turns was also wound on the toroid and connected to a stabilized DC supply to provide the biasing magnetic fields, H , with H being varied over the range 0–13.6 kA m⁻¹.

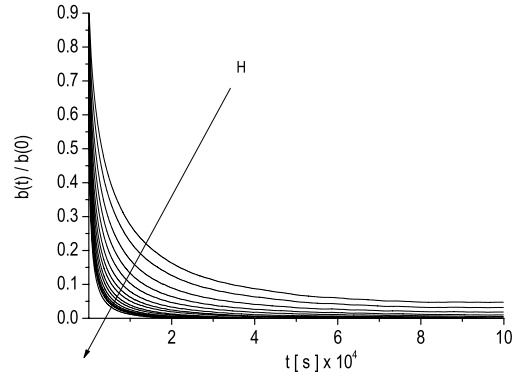


Figure 5. After-effect functions for the data in figure 4.

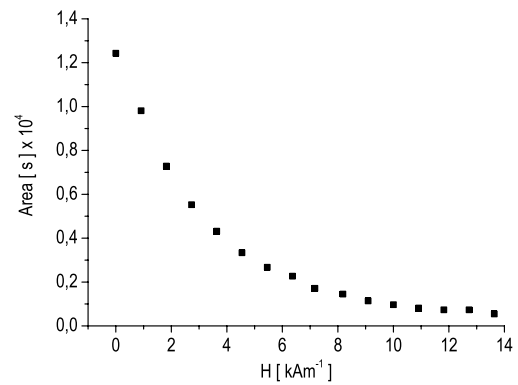


Figure 6. Plot of the area under the after-effect curves as a function of the polarizing field, H .

Figure 4 shows sixteen plots of $\chi''(\omega, H)$ against $\omega/2\pi = f$ (Hz), obtained for the sample over the polarizing field range with the frequency of the maximum, f_{max} , varying from 790 Hz to 22.4 kHz. The corresponding values of the relaxation times, τ_{meas} , were determined by means of equation (8).

The after-effect functions were then obtained from equation (2) and are shown in figure 5, whilst the corresponding variation in area is given in figure 6. It should be noted that, in this case, τ_{eff} (equation (5)) replaced τ_D , the reason for this substitution being that the Debye model assumes particles of one size whilst the sample investigated has a distribution of particle sizes.

A comparison between τ_{meas} and τ_{calc} was made and is shown in figure 7.

A contributing factor for the differences between τ_{calc} and τ_{meas} is the approximation made in the numerical evaluation of the $b(t)$ (see equation (2)) and of the area under the normalized decay curve $b(t)/b(0)$.

An additional possible source of differences between τ_{calc} and τ_{meas} could be effects of interparticle interactions. This could lead to the formation of aggregates, which would affect the value of τ_{meas} .

Another cause for the differences between τ_{calc} and τ_{meas} is the presence of a particle size distribution in the magnetic fluid. This may be explained as follows. Assuming the magnetic fluid to be a linear system, for which the superposition principle applies, its susceptibility is a sum of individual Debye like

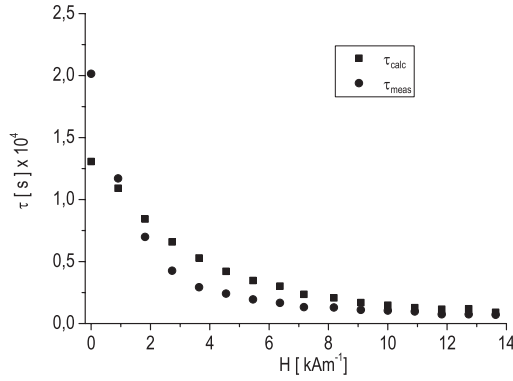


Figure 7. Plot of τ_{meas} and τ_{calc} as a function of polarizing field H for the sample investigated.

susceptibilities of each particle:

$$\chi(\omega) - \chi_{\infty} = \sum_j \frac{A_j(\chi_{0,j} - \chi_{\infty,j})}{1 + j\omega\tau_j} \quad (14)$$

where A_j is the spectral amplitude of particles having the diameter d_j , $\chi_{0,j}$ is the low frequency susceptibility of particles having a diameter d_j , $\chi_{\infty,j}$ is the high frequency susceptibility of particles having a diameter d_j and τ_j is their relaxation time. It follows that the decay or after-effect function, $b(t)$, of the magnetic fluid is a sum of Debye like after-effect functions:

$$b(t) = \sum_j A_j b(0)_j \exp\left(-\frac{t}{\tau_j}\right) \quad (15)$$

where $b(0)_j = \chi_{0,j} - \chi_{\infty,j}$. In this case, the relaxation time evaluated from the area under the normalized after-effect function is

$$\tau_{\text{eff}} = \int_0^{\infty} \frac{b(t)}{b(0)} dt = \frac{\sum_i A_i b(0)_i \tau_i}{\sum_i A_i b(0)_i}. \quad (16)$$

ω_{max} , at which the imaginary part of equation (14) is a maximum, results by solving the equation $\frac{d\chi''}{d\omega} = 0$, i.e.,

$$\sum_j \frac{A_j \tau_j (1 - \omega^2 \tau_j^2)}{(1 + \omega^2 \tau_j^2)^2} = 0. \quad (17)$$

It is obvious that $\omega = \tau_{\text{eff}}^{-1}$ (where τ_{eff} is given by equation (16)) is not a solution of equation (17). Consequently, in the case of a system with a particle size distribution, the relaxation time, τ_{meas} , as determined by means of equation (8) cannot be equal to the relaxation time, τ_{calc} , obtained by

evaluation of the area under the normalized after-effect function.

5. Conclusions

The motivation of this work was a wish to determine the relationship between the area (B) under the after-effect function of a ferrofluid and its dynamic properties. A simple model presented shows that the normalized value, $B/b(0)$, was in fact equal to the Debye relaxation time, τ_D , for systems with a single relaxation time. For the theoretical Debye case, a comparison between τ_D and $\tau_m = 1/(2\pi f_{\text{max}})$ against H , as given in figure 3, shows them to be almost identical, thereby confirming the validity of the model.

In the case of complex susceptibility data obtained for the sample investigated, a discrepancy was shown to exist between the values of the two relaxation times, τ_{calc} and τ_{meas} . A factor contributing to this error was the fact that the data were measured over a truncated frequency range, which resulted in an inaccuracy in the calculation of the parameter B and hence in $B/b(0)$; there was also the fact that the Debye model does not allow for the existence of a particle size distribution, or for the interparticle interactions.

Acknowledgments

Acknowledgment is due to BKP Scaife for useful discussions and also to ESA for the funding of this work.

References

- [1] Scaife B K P 1989 *Principles of Dielectrics* (Oxford: Clarendon)
- [2] Fannin P C 1998 *Advances in Chemical Physics* vol 104, ed I Prigogine and S A Rice (New York: Wiley)
- [3] Brown W F 1963 *J. Appl. Phys.* **34** 1319
- [4] Néel L 1949 *Ann. Geophys.* **5** 99
- [5] Keller E and Wohlfarth E P 1966 *J. Appl. Phys.* **37** 4816
- [6] Shliomis M I and Raikher Yu L 1980 *IEEE Trans. Magn. Mag.* **16** 237
- [7] Shliomis M I 1974 *Sov. Phys.—Usp.* **17** 53
- [8] Debye P 1929 *Polar Molecules* (New York: Chemical Catalog Company)
- [9] Fannin P C, Scaife B K P, Giannitsis A T and Charles S W 2002 *J. Phys. D: Appl. Phys.* **35** 1305
- [10] Fannin P C, Scaife B K P and Charles S W 1988 *J. Phys. D: Appl. Phys.* **21** 533
- [11] Raikher Yu L and Shliomis M I 1994 *Adv. Chem. Phys.* **87** 595 (chapter 8)
- [12] Fannin P C, Scaife B K P and Charles S W 1986 *J. Phys. E: Sci. Instrum.* **19** 238